ScientificScholar®
Knowledge is power
Publisher of Scientific Journals

www.apospublications.com

APOS Trends in Orthodontics

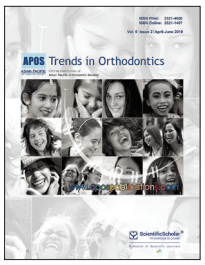

Original Article

Influence of printing procedure and printing axis of dental alloys on dimensional accuracy, surface roughness, and porosity

Simon Graf[1]*, Moritz Berger[1]*, Nadja Rohr[1]

[1]Biomaterials and Technology, Department of Research, University Center of Dental Medicine Basel, Basel, Switzerland.
*The first two authors have equally contributed to the manuscript.

***Corresponding author:**
Nadja Rohr,
Biomaterials and Technology,
Department of Research,
University Center of Dental
Medicine Basel, Basel,
Switzerland.

nadja.rohr@unibas.ch

Received: 17 February 2022
Accepted: 28 March 2022
EPub Ahead of Print: 21 June 2022
Published: 16 September 2022

DOI
10.25259/APOS_27_2022

Quick Response Code:

ABSTRACT

Objectives: This study aimed to evaluate the printing procedure and printing axis and its influence on the dimensional accuracy, surface roughness, porosity, and strength of 3D-printed dental alloys used in orthodontics prepared using binder jetting (BJ), electron beam melting (EBM), or selective laser melting (SLM).

Material and Methods: Specimens with a dimension of 50 mm × 12 mm were produced using BJ, EBM, and SLM techniques of dental alloys and were printed either along the X-, Y-, or Z-axis (n = 8 per group). Specimen dimension was chosen according to the ISO standard 6892-1 for tensile strength test specimens. Surface roughness parameters Sa, Sz, Sq, and Ssk were obtained using a 3D laser microscope and porosities were visualized with scanning electron microscopy (SEM). The specimen surfaces were optically scanned and volumetric deviations from the original stereolithography files were calculated. Afterward, tensile strength was measured.

Results: The printing method and printing axis significantly affected surface roughness parameters ($P < 0.05$). Overall, the lowest surface roughness Sa values were found for BJ (9.1 ± 3.4 µm) followed by SLM (39.8 ± 24.2 µm) and EBM (50.4 ± 6.4 µm). BJ showed the smallest dimensional deviation followed by EBM and SLM. SEM analysis revealed a porous structure of BJ while fewer pores were observed on EBM and SLM samples. The ultimate tensile strength was only determined for BJ (495 ± 6 MPa) and EBM (726 ± 50 MPa) as the strength of SLM superseded the strength of the holder of the universal testing machine.

Conclusion: BJ printing provides the highest dimensional accuracy with the smoothest surfaces irrespective of the printing axis. However, the remaining porosities owed to this printing procedure may have decreased the strength of the material.

Keywords: 3D-Printing, Orthodontics, Binder-jetting, Selective laser melting, Electron beam melting

INTRODUCTION

Computer-aided design and computer-aided manufacturing are increasingly used in dentistry, especially in orthodontics.[1] 3D printing is currently mainly used to produce models with resin materials but is also available for removable dental prostheses,[2-4] oral splints,[5] drilling templates,[6] or orthodontic appliances.[7-11] To process dental alloys for the framework of removable dental prostheses or orthodontic appliances, different printing processes are currently available. The first printing technique used for the processing of metal alloys was selective laser sintering (SLS). Metal particles are partially melted in layers of 20–100 µm and are subsequently reheated and completely joined, resulting in volumetric differences.[12] SLS has, therefore, been

replaced by selective laser melting (SLM), where particles are already fused within the first step. Another approach is electron beam melting (EBM), where metal powder is melted using an electron beam instead of a laser source. In contrast to those technologies joining pure metal alloy powders, another approach deposits a binder over metal powder layers. This so-called binder jetting (BJ) technique requires additional curing steps involving depowdering, sintering imperfections, and annealing of the object.[13] The printing technique may result in varying mechanical properties due to insufficiently fused particles and incorporated porosities.[12-15] Furthermore, the production time of printed specimens is highly dependent on the chosen printing method and the required post-processing procedures. Even when selecting the same printing procedure but a different printer model, the outcome may vary. Factors influencing the outcome are the size of the building platform (chamber), the temperature within the chamber, laser energy (melting temperature), printing speed, or layer thickness.[14-20]

Dental materials that are placed within the oral cavity over a longer period should have a smooth surface with a surface roughness value Ra <0.2 μm to prevent biofilm accumulation.[21]

From 3D printing with resin materials, it is known that the positioning of the specimens on the building platform influences its mechanical properties[22] and printing accuracy.[17] For metal processing, the influence of the positioning of a specimen on the building platform on dimensional accuracy, surface roughness, and porosities is still unclear. The purpose of this study was therefore to compare specimens produced using either BJ, EBM, or SLM in three printing axes (X-, Y-, and Z-axis) to the original stereolithography (STL) file. Null hypotheses were that (1) the printing method does not affect dimensional accuracy and surface roughness and (2) the printing axis does not affect dimensional accuracy and surface roughness.

MATERIAL AND METHODS

Specimen production

Specimens with a dimension of 50 mm × 12 mm were produced using BJ, EBM, and SLM techniques and were printed either along the X (Group III), Y (Group II), or Z-axis (Group I) [Table 1 and Figure 1] (n = 8 per group). Specimen dimension was chosen according to the ISO standard 6892-1 for tensile strength test specimens. Unfortunately, it was not possible to process the same alloy with varying printing procedures.

BJ specimens were produced out of 316L steel with a DM P2500 (Digitalmetal, Höganas, Sweden). Specimens were built in layers of 42 μm with a binding material without supporting structures at room temperature. Afterward, the residual powder was removed and specimens were sintered. Printing time for a thickness of 2 mm was 50 min plus additional curing-, debinding, and sintering accumulating to 24 h.

Table 1: Specimens produced with either BJ, EBM, or SLM in three different printing axis along each axis (X, Y, and Z).

Code	Processing	Printing axis	Material	Company
BJ I	Binder	Z-axis	316L steel	Digital Metal
BJ II	jetting	Y-axis	(Fe, Cr, Ni,	AB, Höganäs
BJ III		X-axis	Mo, C)	(Sweden)
EBM I	Electron	Z-axis	Arcam	GE Additive,
EBM II	beam	Y-axis	CoCrMo	Concept Laser,
EBM III	melting	X-axis	Powder	Lichtenfels (Germany)
SLM I	Selective	Z-axis	CoCr	CAD/Tools,
SLM II	laser	Y-axis	Remanium	Augsburg
SLM III	melting	X-axis	Star	(Germany)

BJ: Binder jetting, EBM: Electron beam melting, SLM: Selective laser melting

EBM specimens were produced with cobalt chrome molybdenum (CoCrMo) powder on an Arcam EBM spectra L (GE Additive, Lichtenfels, Germany). The building chamber was heated just below the melting point of the powder under a vacuum. The printing time of a 2 mm structure was 7 min, but the complete process with heating up and cooling down took 4 h. No supportive structures were needed, as the whole building chamber is heated up just below the melting point of the chosen material.

SLM specimens were produced of CoCr at the laboratory of concept laser (Lichtenfels, Germany, run by Caddent, Germany). This device can print 50–100 layers of 0.03 mm within 14 h. A layer of metal powder is, therefore, distributed evenly on a building platform. Layers are fused with a laser beam. The complete build-up platform lowers for the next layer to be distributed on the complete platform. As every melted part starts to cool when the laser moves on, shrinking occurs and stress is induced. To release tension out of the final product, further heat-treatment of 1 h at 1140°C was required. To reduce shrinkage, a supporting structure was attached to the edges of the triangular structure of the specimens. After specimen production, supporting structures were removed but no additional polishing steps were performed.

Surface roughness

Surface roughness parameters were obtained using a 3D laser microscope (VKX-1050, Keyence, Tokyo, Japan). The following parameters were obtained on three specimens per group (n = 3) with a 10x objective over an area of 4600 μm × 3400 μm on the largest side of the specimens after the application of a Gaussian low-pass filter of 80 μm:

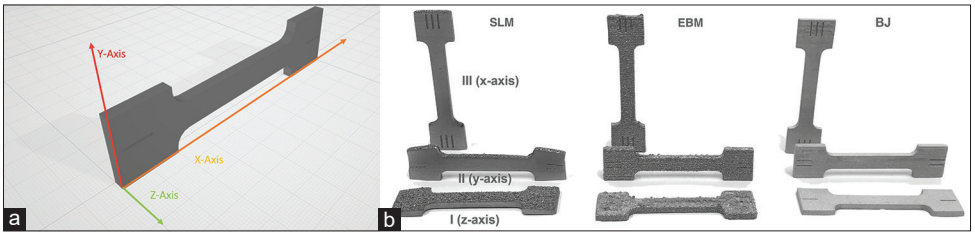

Figure 1: (a) Specimen printing direction in X-, Y-, and Z-axis). (b) Specimens of SLM, electron beam melting, and binder jetting.

Sa: Difference in height of each point compared to the arithmetical mean of the surface
Sz: Sum of the value of the highest peak and the deepest trough within a defined area
Sq: Root mean square value of ordinate values within the defined area. It is equivalent to the standard deviation of heights
Ssk: Represents the degree of bias of the roughness shape (asperity)

Dimensional accuracy

The specimens were optically scanned (HandyScan BLACK Elite, AMETEK GmbH Division Creaform Leinfelden-Echterdingen, Germany) with a scan-precision of ± 0.020 mm + 0.040 mm/m (n = 2 per group). The stl-files derived from the scan were fit to the original stl file of the specimens (VXInspect 3D testing software, AMETEK GmbH Division Creaform Leinfelden-Echterdingen, Germany) according to the best-fit method. The minimal and maximal deviation and standard deviation from 0 in mm from the original stl-file were calculated.

Porosity

Surfaces of one specimen per group were polished using silicon carbide paper grit P400, P800, P1200, and diamond paste of 3 µm. Specimens were then etched with a solution of H_2O_2 and hydrochloric acid 37% to reveal the structure and potential porosities. Surfaces were then analyzed using scanning electron microscopy (ESEM XL-30, Philips, Eindhoven, The Netherlands) at 20 kV in SE mode.

Tensile strength measurement

Specimens (n = 6) were fixed in a customized holding device in a universal testing machine (Z020, Zwick/Roell, Ulm, Germany). Tensile strength testing was performed according to the ISO standard 6892-1. The ultimate tensile strength (R_m) was recorded.

Statistical analysis

For surface roughness parameters, mean and standard deviations were calculated. Groups were tested for normal distribution using Shapiro–Wilk test and compared using two-way ANOVA to test for the effect of printing method and printing axis followed by Fisher LSD *post hoc* test (α = 0.05). To analyze dimensional accuracy, Student's t-test was used to compare differences between groups (α = 0.05).

RESULTS

Surface roughness

The surface roughness measurements with statistics are displayed in [Table 2]. Two-way ANOVA revealed a significant effect of printing method and printing axis for all roughness parameters (all $P < 0.001$, Ssk axis $P = 0.025$). Mean Sa values for the different printing procedures ranged for BJ I 5.9 to BJ II 12.88 µm, for EBM II 47.48 to EBM I 52.2 µm, and for SLM II 21.9 to SLM I 71.77 µm. For Sz, the mean values were for BJ I 60.67 to BJ II 121.39 µm, for EBM II 449 to EBM I 535.46 µm, and for SLM 131.55 III to SLM I 579.45 µm. The Lowest Sa and Sz values were revealed for specimens printed with the BJ I method. *Post hoc* tests showed no significant effect of the printing axis for BJ and EBM ($P > 0.05$). While for SLM roughness values, Sa and Sz were significantly higher for Group I compared with III and II ($P < 0.001$).

For BJ specimens, a homogeneous surface with few and very regular depths and heights of the troughs and peaks is observable in [Figure 2]. For EBM all groups and SLM I, an irregular height distribution is visible, and the surface is dotted with peaks and troughs at irregular intervals. SLM II and SLM III appear smoother than SLM I, confirming roughness measurements.

Dimensional accuracy

[Figure 3] shows the dimensional deviation of the specimens compared with the original STL-file using different colors. Green indicates a precise print. Negative deviations are indicated in blue. Additive deviations are given in red. Most accurate specimen dimensions were achieved with BJ-process followed by EBM and then SLM.

Deviations were quantified in [Figure 4]. BJ showed the smallest deviation with no significant differences between the printing axis ($P > 0.05$). Significantly larger deviations were recorded for EBM I and II that did not vary significantly

Table 2: Surface roughness parameters mean and standard deviation of BJ, EBM, and SLM (n=3 per group).

Group	Sa (µm)	Sz (µm)	Sq (µm)	Ssk
BJ I	5.90±1.06^{A}	60.67±4.47^{A}	7.33±1.25^{A}	-0.196±0.05^{A}
BJ II	12.88±2.51^{A}	121.39±10.73^{A,B}	16.14±2.73^{A,B}	0.33±0.09^{B}
BJ III	8.65±0.83^{A}	93.13±7.59^{A,B}	10.84±1.04^{A}	0.027±0.16^{A}
EBM I	52.2±2.81^{B}	535.46±66.99^{C,D}	72.37±5.13^{C}	1.36±0.15^{C}
EBM II	47.48±8.24^{B}	449.18±69.21^{D}	60.18±9.38^{D}	0.52±0.36^{B}
EBM III	51.44±8.38^{B}	455.44±51.29^{D}	63.61±9.68^{C,D}	0.27±0.18^{B}
SLM I	71.77±0.93^{C}	579.45±38.84^{C}	91.91±1.32^{E}	0.15±0.08^{A,B}
SLM II	21.9±0.1^{D}	157.04±30.61^{B}	26.16±1^{B,F}	-0.320±0.5^{A}
SLM III	25.88±5.56^{D}	131.55±22.28^{A,B}	29.93±6.46^{F}	-0.08±0.04^{A,B}
ANOVA				
Printing method	P<0.001	P<0.001	P<0.001	P<0.001
Printing axis	P<0.001	P<0.001	P<0.001	P=0.025

P-values obtained with two-way ANOVA for each effect are displayed. Differences within subgroups tested with Fisher LSD test are indicated with varying superscript letters (P<0.05). BJ: Binder jetting, EBM: Electron beam melting, SLM: Selective laser melting

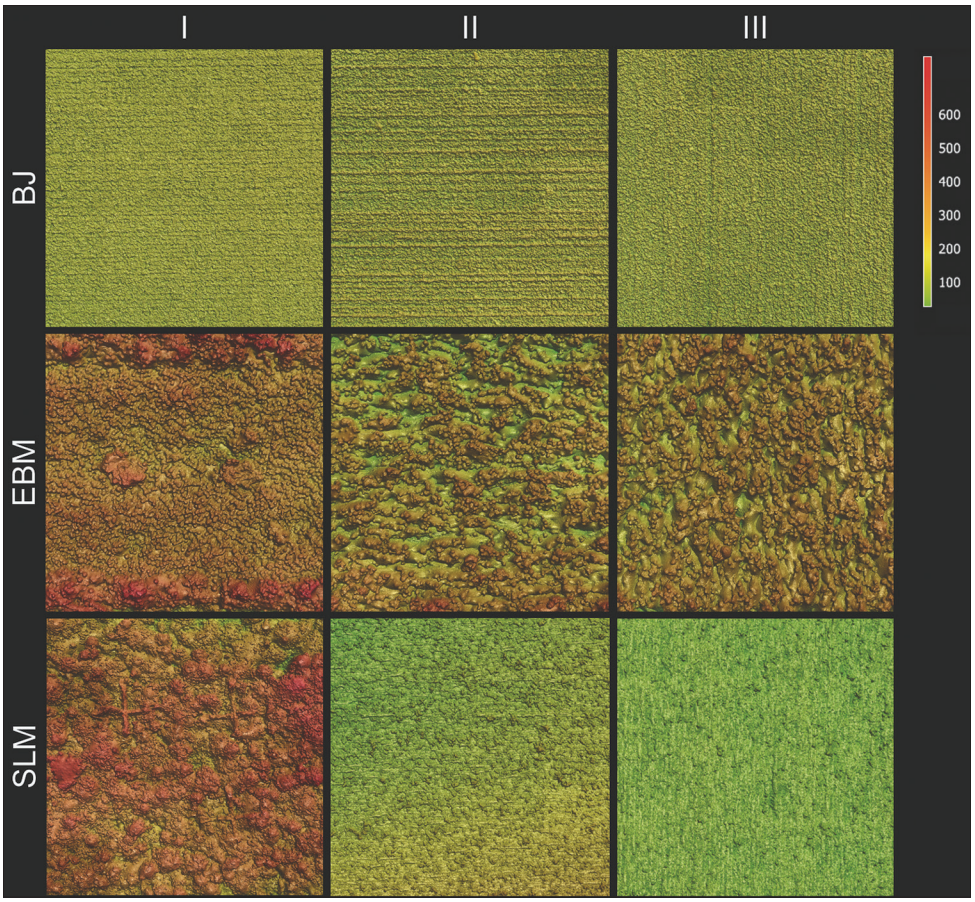

Figure 2: Surface topography of binder jetting (BJ), selective laser melting, and BJ (×10 objective, image size 4600 µm × 3400 µm, scale in µm).

from each other (P = 0.433), compared with EBM III (both P < 0.001). SLM was the least accurate printing method displaying low dimensional accuracy with significantly higher discrepancies for SLM I than for II and III (all P < 0.001).

Porosity

Scanning electron microscopic images are displayed in [Figure 5]. BJ samples were the most porous. Large holes and a diffuse non-homogeneous surface can be observed. The EBM

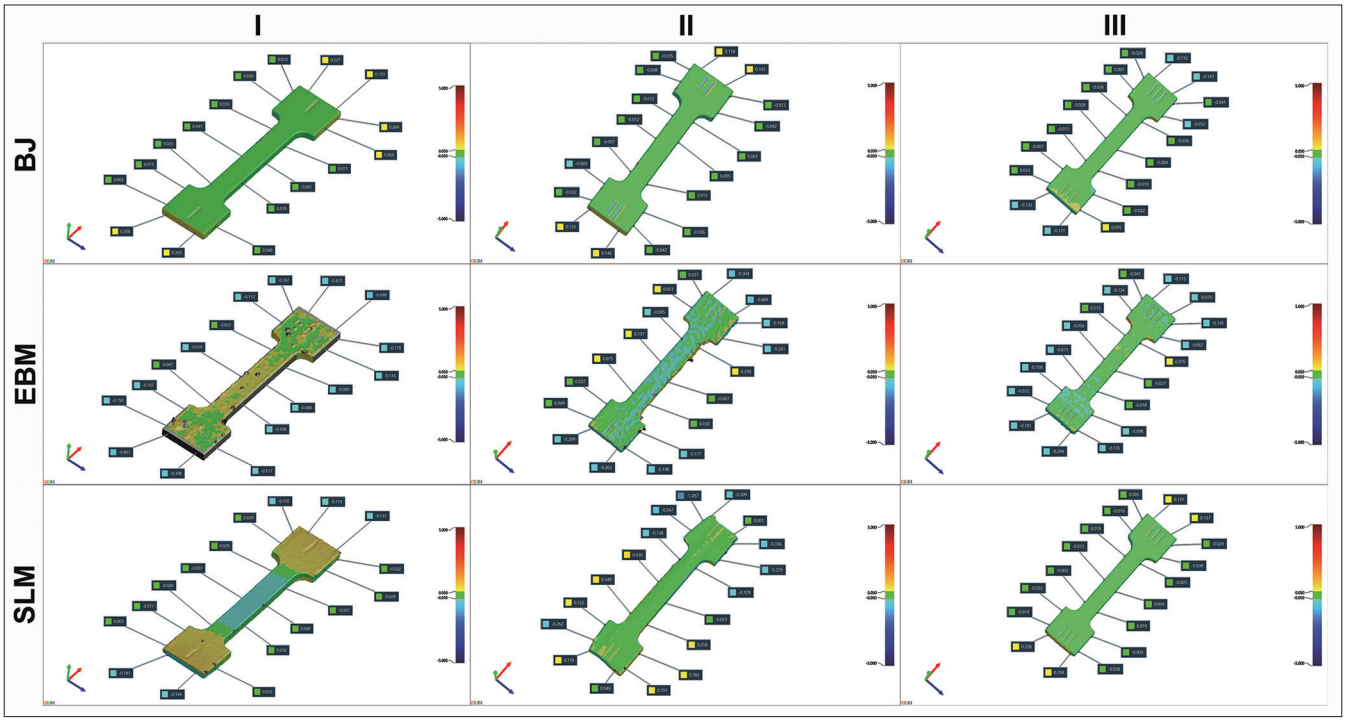

Figure 3: Dimensional accuracy visualization of the specimens. Green indicates a high conformity with the original file used for printing.

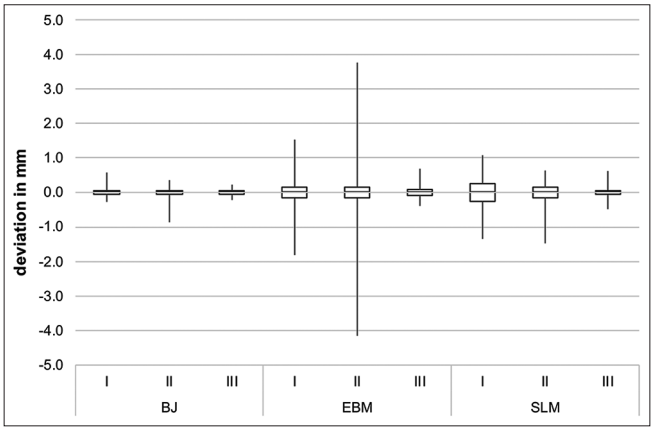

Figure 4: Dimensional deviation in mm of the specimens from the original stl using best fit comparison (boxplot indicate standard deviation and min/max, mean = 0) (n = 2 per group).

process is less porous. Various precipitates are visible. For SLM specimens, the various porous cluster can be seen in the image, surrounded by a homogeneous non-porous surface.

Tensile strength

The ultimate tensile strength could only be determined for the complete set of BJ and EBM I and II specimens due to the high strength of the EBM III and SLM specimens that did not rupture with the applied method. Consequently, no statistical comparison was performed. R_m was as follow: BJ I: 505 ± 5 MPa, BJ II: 489 ± 9 MPa, BJ III: 490 ± 3 MPa, EBM I: 730 ± 51 MPa, and EBM II: 723 ± 49 MPa.

DISCUSSION

This study aimed to evaluate the null hypotheses that (1) the printing method does not affect dimensional accuracy and surface roughness and (2) the printing axis does not affect dimensional accuracy and surface roughness to estimate the potential of additive manufacturing in orthodontic dentistry. Both printing method and printing axis affected surface roughness parameters, dimensional accuracy as well as porosities, and tensile strength values. Therefore, the null hypotheses (1) and (2) were both rejected.

The surface roughness measurements revealed that with BJ processing, the most homogeneous surface was achieved. EBM and SLM processes created a rather rough and wavy surface that requires further post-processing to obtain a smooth surface finish and accurate dimensions. Surfaces of materials that are placed in the oral cavity require a surface with a roughness value of Ra < 0.2 µm to prevent biofilm accumulation.[21] As Sa values of all tested specimens superseded this threshold value, further polishing is recommended after all printing procedures. Most manufacturers of orthodontic appliances add extra volume that is later polished off during a post-printing procedure, resulting in the final dimension of the planned product. The different polishing processes are either by hand, automated

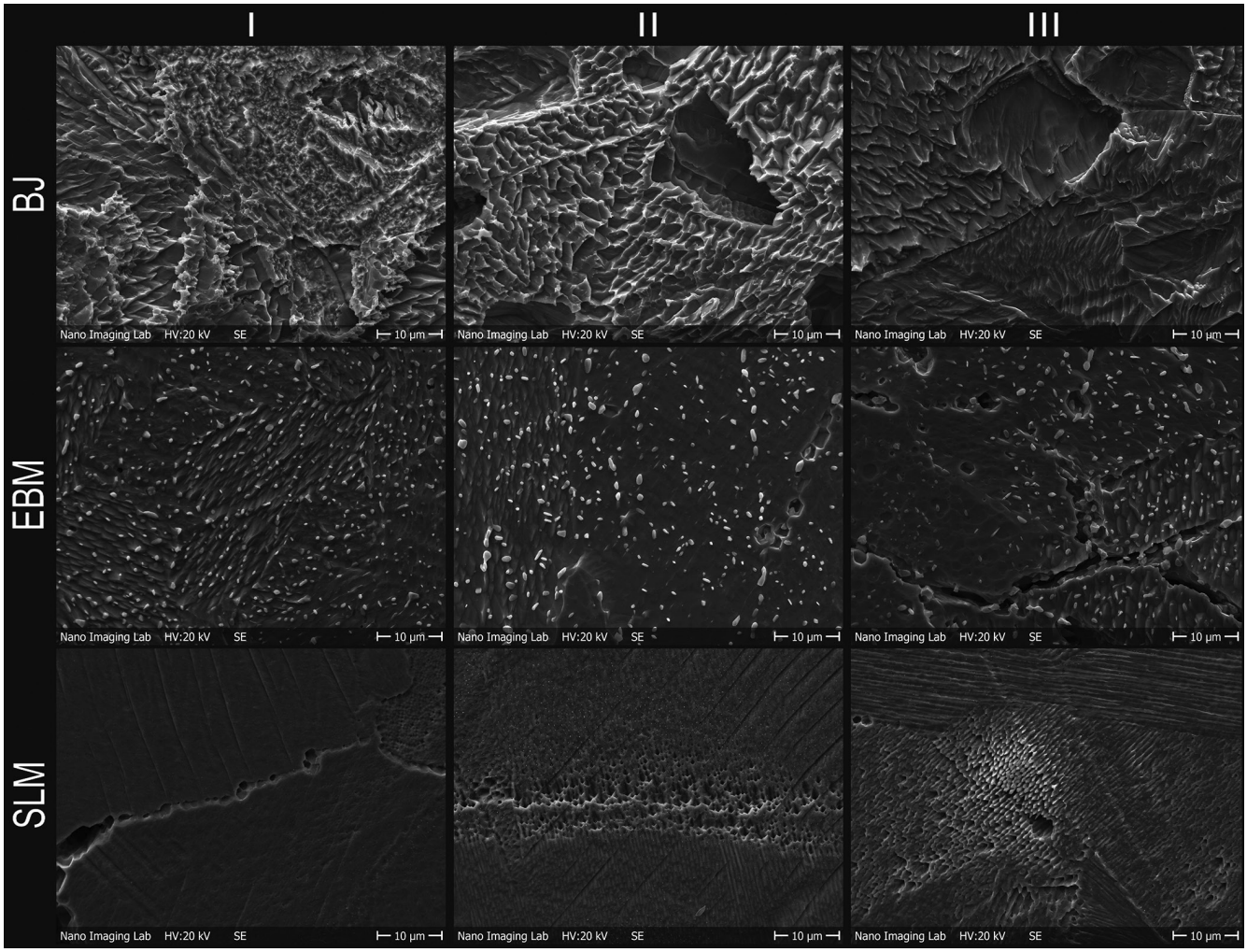

Figure 5: Scanning electron microscopy images (magnification bar: 10 µm) of polished and etched specimens printed using binder jetting, electron beam melting, and selective laser melting technique in three different printing axes.

with polishing machines, or electrochemical. Manufacturers are encouraged to improve the surface quality of EBM and SLM to limit extensive post-processing.

The printing axis did affect the surface roughness of the specimens as well. Overall, the lowest surface roughness was achieved using printing axis II > III > I. Hence, the largest surface area of a specimen should not be placed parallel to the printing axis when a smooth surface finish is to be achieved.

When analyzing the dimensional accuracy, it was observed that all specimens within all processes and axis displayed a certain deviation. Using printing method BJ, the lowest discrepancies were found. With EBM processing deviation was larger and worst with SLM. Printing SLM in axis III provided accurate specimens while for I and II, the deviation was not acceptable. Another study that examined trifurcated 3D printed 316L steel joints using SLM processing showed that maximal discrepancies were < 5%.[23]

As specially the printing axes I and II showed the highest deviations, it might be necessary to avoid printing large solid volumes. During the cooling process, the solid specimens may deform due to their weight. Rather small volumes or cooling channels within the printed body might be a useful tool to be further investigated.

Although BJ displayed the best surface roughness properties and dimensional accuracy, unfortunately, high porosity was observed in SEM images. Manufacturers are encouraged to improve these porosities as BJ processing is the least expensive (BJ CoCr). Furthermore, tensile strength values of BJ were lower than for EBM and probably SLM which superseded the limit of the testing machine. However, the tensile strength values may have been influenced by the different materials used for the printing methods, which is a limitation of this study. It has been found that CoCr alloy specimens processed by SLM technique mechanical properties (ultimate tensile strength 1158 ± 10 MPa and

Figure 6: An example of printed orthodontic appliances for clinical application with support structures using selective laser melting technique.

Vickers hardness 399 ± 24 HV) were improved compared with specimens prepared by casting and milling techniques. Hence, SLM printing provided a microstructure with relatively homogeneously distributed fine grains and more second-phase particles, which can significantly increase strength.[24] Another study compared EBM and SLM using a CoCr alloy for metallic orthopedic implant applications. Tensile strength values of 562–884 MPa for SLM and 960 MPa for EBM were recorded.[25]

All three printing methods have their advantages. SLM is currently the most common method applied in orthodontics, despite its accuracy and surface deficiencies observed in this study. However, the design of orthodontic appliances is much more filigree than that of the tested specimens in this study. Orthodontic appliances are printed using supportive structures that allow faster cooling without deformation [Figure 6]. The production of larger test specimens for tensile strength testing used in this study may have caused greater deformations. Hence, further studies may be conducted to measure printing accuracy with more clinically relevant specimen dimensions. In the long-term, the easiest procedure regarding printing speed, material properties, and pre-and post-processing will find its way to in-house 3D metal printing in dental and orthodontic clinics.

CONCLUSION

Within the limitations of this study, it can be concluded that with the BJ printing method of a dental alloy, the highest dimensional accuracy with smoothest surfaces, irrespective of the printing axis was achieved. EBM and SLS processes created rather rough and wavy surfaces that required further post-processing to obtain a smooth surface finish and accurate dimensions. Those two printing techniques were highly affected by varying the printing direction.

Declaration of patient consent

Patient's consent not required as there are no patients in this study.

Financial support and sponsorship

Nil.

Conflicts of interest

There are no conflicts of interest.

REFERENCES

1. Bhargav A, Sanjairaj V, Rosa V, Feng LW, Yh JF. Applications of additive manufacturing in dentistry: A review. J Biomed Mater Res B Appl Biomater 2018;106:2058-64.
2. Venkatesh KV, Nandini VV. Direct metal laser sintering: A digitised metal casting technology. J Indian Prosthodont Soc 2013;13:389-92.
3. Wu M, Tinschert J, Augthun M, Wagner I, Schädlich-Stubenrauch J, Sahm PR, *et al.* Application of laser measuring, numerical simulation and rapid prototyping to titanium dental castings. Dent Mater 2001;17:102-8.
4. Soltanzadeh P, Suprono MS, Kattadiyil MT, Goodacre C, Gregorius W. An *in vitro* investigation of accuracy and fit of conventional and CAD/CAM removable partial denture frameworks. J Prosthodont 2019;28:547-55.
5. Perea-Lowery L, Gibreel M, Vallittu PK, Lassila L. Evaluation of the mechanical properties and degree of conversion of 3D printed splint material. J Mech Behav Biomed Mater 2021;115:104254.
6. Wes JT, Houppermans PN, Verweij JP, Mensink G, Liberton N, van Merkesteyn JP. The 3D printed drilling template for bilateral sagittal osteotomy. Ned Tijdschr Tandheelkd 2016;123:400-4.
7. Graf S, Cornelis MA, Hauber Gameiro G, Cattaneo PM. Computer-aided design and manufacture of hyrax devices: Can we really go digital? Am J Orthod Dentofac Orthop 2017;152:870-4.
8. Graf S. Direct printed metal devices the next level of computer-aided design and computer-aided manufacturing pplications in the orthodontic care. APOS Trends Orthod 2017;7:253-9.
9. Graf S, Vasudavan S, Wilmes B. CAD-CAM design and 3-dimensional printing of mini-implant retained orthodontic appliances. Am J Orthod Dentofac Orthop 2018;154:877-82.
10. Graf S, Vasudavan S, Wilmes B. CAD/CAM metallic printing of a skeletally anchored upper molar distalizer. J Clin Orthod 2020;54:140-50.
11. Ghislanzoni LH, Negrini S. Digital lab appliances: The time has come. J Clin Orthod 2020;54:562-9.
12. Oyar P. Laser sintering technology and balling phenomenon. Photomed Laser Surg 2017;36:72-7.
13. Li M, Du W, Elwany A, Pei Z, Ma C. Metal binder jetting additive manufacturing: A literature review. J Manuf Sci Eng 2020;142:090801.
14. Kim JH, Kim MY, Knowles JC, Choi S, Kang H, Park SH,

et al. Mechanophysical and biological properties of a 3D-printed titanium alloy for dental applications. Dent Mater 2020;36:945-58.
15. Bae S, Hong MH, Lee H, Lee CH, Hong M, Lee J, *et al*. Reliability of metal 3D printing with respect to the marginal fit of fixed dental prostheses: A systematic review and meta-analysis. Materials 2020;13:4781.
16. Aretxabaleta M, Xepapadeas A, Poets C, Koos B, Spintzyk S. Fracture load of an orthodontic appliance for robin sequence treatment in a digital workflow. Materials 2021;4:344.
17. McCarty MC, Chen SJ, English JD, Kasper F. Effect of print orientation and duration of ultraviolet curing on the dimensional accuracy of a 3-dimensionally printed orthodontic clear aligner design. Am J Orthod Dentofacial Orthop 2020;158:889-97.
18. Presotto AG, Barão VA, Bhering CL, Mesquita MF. Dimensional precision of implant-supported frameworks fabricated by 3D printing. J Prosthet Dent 2019;122:38-45.
19. Khaledi AA, Farzin M, Akhlaghian M, Pardis S, Mir N. Evaluation of the marginal fit of metal copings fabricated by using 3 different CAD-CAM techniques: Milling, stereolithography, and 3D wax printer. J Prosthet Dent 2020;124:81-6.
20. Braian M, Jönsson D, Kevci M, Wennerberg A. Geometrical accuracy of metallic objects produced with additive or subtractive manufacturing: A comparative *in vitro* study. Dent Mater 2018;34:978-93.
21. Bollen CM, Lambrechts P, Quirynen M. Comparison of surface roughness of oral hard materials to the threshold surface roughness for bacterial plaque retention: A review of the literature. Dent Mater 1997;13:258-69.
22. Kotzem D, Arold T, Niendorf T, Walther F. Influence of specimen position on the build platform on the mechanical properties of as-built direct aged electron beam melted Inconel 718 alloy. Mater Sci Eng A 2020;772:138785.
23. He P, Du W, Wang L, Kiran R, Yang M. Additive manufacturing and mechanical performance of trifurcated steel joints for architecturally exposed steel structures. Materials 2020;13:1901.
24. Zhou Y, Li N, Yan J, Zeng Q. Comparative analysis of the microstructures and mechanical properties of Co-Cr dental alloys fabricated by different methods. J Prosthet Dent 2018;120:617-23.
25. Sing SL, An J, Yeong WY, Wiria FE. Laser and electron-beam powder-bed additive manufacturing of metallic implants: A review on processes, materials and designs. J Orthop Res 2016;34:369-85.

How to cite this article: Graf S, Berger M, Rohr N. Influence of printing procedure and printing axis of dental alloys on dimensional accuracy, surface roughness, and porosity. APOS Trends Orthod 2022;12:149-56.